CLM-P773

CLM-P773

UKAEA

Preprint

GIRTH WELDING OF X-60 PIPELINE WITH A 10kW LASER

CULHAM LABORATORY
LIBRARY
11 JUL 1986
b

J. H. P. C. MEGAW
M. HILL
S. J. OSBOURN

CULHAM LABORATORY
Abingdon, Oxfordshire

1986

This document is intended for publication in a journal or at a conference and is made available on the understanding that extracts or references will not be published prior to publication of the original, without the consent of the authors.

Enquiries about copyright and reproduction should be addressed to the Librarian, UKAEA, Culham Laboratory, Abingdon, Oxon. OX14 3DB, England.

CLM-P773

GIRTH WELDING OF X-60 PIPELINE WITH A 10kW LASER

J.H.P.C. Megaw, M. Hill & S.J. Osbourn

UKAEA Culham Laboratory, Abingdon, Oxfordshire, OX14 3DB, UK.

Abstract

Single-pass autogeneous welding by 10kW laser of API 5LX X60 pipeline samples, of 760mm diameter and with wall thickness up to 19mm, in a configuration appropriate to J-lay operations, is described. The results of mechanical testing, including Charpy impact properties and their dependence on process conditions, are presented and discussed.

To be published in the proceedings of the SPIE/ANRT Conference on High Power Lasers and Their Industrial Applications, Innsbruck, 15-18th April 1986.

APRIL 1986

Introduction

Present off-shore pipe-laying operations utilise a barge on which the horizontal pipe-lengths being joined are passed through several stations where arc-based welding passes (with filler) are sequentially carried out. The welded pipe, as it passes off the end of the barge and down to and along the sea-bed, has a shape which gives the method its name, the S-laying technique. In the near future, and particularly in deep water, it is anticipated that increasing use will be made of an arrangement whereby pipes, supported vertically, are joined on the barge and passed down to the sea-bed in a J-shaped curve. Sequential welding in a number of stations is clearly now less attractive and the industry is interested in alternative welding processes which could, in a single station, maintain high laying-rates whilst de-skilling and improving quality of welding. The industry is therefore actively investigating 'new' processes such a flash-butt[1], friction[2], electron-beam[3] and laser welding.

The objective of this paper is to report some of the results from laboratory-based experimental investigations of the laser welding of X-60 pipeline steel in diameters up to 760mm and wall thicknesses up to 19mm. The emphasis here is on the characteristics and properties in single-pass, autogeneous welds carried out with the pipe axis vertical.

Experimental Programme

Figure 1 shows the Culham CL10 10kW laser installation. The laser[4] is a transverse-flow, DC electrically-excited device. It consists of two modules arranged end-to-end to permit operation with an unstable resonator, of magnification M=3, containing a single roof-top fold. Much of the work described here was performed shortly after the initial commissioning of the laser when it was fitted with a zinc-selenide window. It was subsequently found that thermal lensing of that window was causing optical degradation of the beam and it was replaced by an aerodynamic window yielding significant improvement in weld penetration capability[5].

The laser output beam is approximately 45mm diameter and can be switched to any one of three workstations. Workstation 1, shown on Figure 1, was used for much of the present work and is a compact enclosure containing a fixed focus head which can be oriented to permit downhand or sidehand welding on flat coupons, or sidehand welding on pipe-samples which are rotated about a vertical axis on a large turntable. The second workstation, used in later phases, enables workpieces up to 1 tonne to be manipulated in three axes and the beam delivery system permits welding at any attitude. These arrangements thus permit assessment of J-lay positional welding without the expense, at this stage, of carrying the laser beam around a fixed pipe. In workstation 3, also used later in the programme, the beam is directed down the axis of a large lathe faceplate and then deflected by mirrors, first radially outwards and then axially again before being focused radially inwards on to a fixed pipe sample which is mounted on a tailstock. This arrangement permits assessment of positional welding in S-lay configuration before building optics capable of delivering the beam around a pipe of effectively infinite length.

In this programme the metal mirror focus units used were all of the folded, off-axis Cassegrainian type, most of the work being carried out at f/8 and with focus position chosen to give maximum penetration. Standard Culham gas shrouding[6] was used for all welding. This provided helium control of the plasma plume above the workpiece and helium shrouding of the cooling outer bead so that smooth, uncontaminated welds could be produced routinely. Weld disruption reported in earlier work[7] was not seen. Filler wire, used in later phases, could be fed to the interaction point on the 'upstream' side and at approximately 45° to the beam using the technique developed at Culham previously[8].

The pipeline used was to API 5LX X60. Although it has the rather broad chemical specification shown in Table 1, the material is a high strength, microalloyed, controlled-rolled steel of minimum tensile strength 517 MPa and minimum yield strength of 413 MPa. The analysis of the material used is also given in Table 1.

The present pipes, which had a microstructure of banded ferrite/pearlite with a grain size of approximately 5μm, were of 760mm outer diameter, 19mm wall and contained a longitudinal submerged arc seam weld. Test pieces of lower wall thickness were achieved by machining the pipe bore. Excess wall thickness due to the longitudinal seam weld reinforcement was removed by local hand grinding, and prior to welding the pipe surfaces either side of the joint were dressed to remove surface oxide and contamination. Typically two pipe pieces, each 225mm long and having their longitudinal seams displaced at 180°, could be aligned with respect to each other to average out their non-circularity and yield surface mismatch less than 1mm. They were pulled together by tie bars passing through steel end plates, the assembly being internally flushed with helium before and during welding.

Welding was carried out with approximately 11kW at the work, and with welding speeds of 6mms^{-1}, dropping to 5mms^{-1} at the overlap which extended for approximately 75mm. At the start and end of the weld, beam power was ramped over a time of approximately 20 seconds. The time to weld a 760mm pipe was thus approximately 7 minutes.

Results and Discussion

The following discussion is based on a large number of weld trials carried out on flat coupons and pipe samples. However, many of the detailed test results arose through examination of six particular pipe samples, three each of 17mm and 19mm wall thickness. These samples were destructively tested according to Section 2.6 of the API Standard 1104 which concerns qualification of welding procedures for butt joints in pipeline. Additionally they were assessed by metallography and radiography and for Charpy impact toughness.

Penetration and Weld Cross Sections

For a given beam power, as welding speed is steadily decreased, laser weld penetration increases to a limiting value and may then indeed start to decrease again. At these slow speeds, there is significant growth of the plasma plume above the keyhole which absorbs beam energy and conducts heat to the sides of the weld to make it broader, shallower and less parallel sided. Again for a given beam power, better penetration is achieved for higher beam intensities (smaller focused spots) and for optimised plasma control. Indeed it seems likely that the two are related since, as has been noted for non-vacuum electron beam sources[9], a more finely focused beam may create a hotter channel so that equilibrium pressure can be achieved by higher temperature and therefore lower density of the absorbing species. Nevertheless additional means of plasma control are normally required and the growth of the plume may be controlled by directing at it a jet of inert gas having high ionisation potential (such as helium) and having flow and pressure distributions which assist in the formation of the keyhole and in convective cooling of the plasma. In particular at slow welding speeds careful adjustment of plasma control is necessary.

These comments are particularly relevant to the single pass welding of 19mm wall thickness. It was found that, with a ZnSe window on CL10, the limit of penetration with 11kW at the work was approximately 19mm at a welding speed of 5 to 6mms^{-1}. That is, although full penetration welds were achievable, (i) the inner beads were less full than desirable and (ii) substantial plasma broadening of the weld crown occurred. These features are shown on Figure 2 where it is seen that the tapering cross-section imposed an alignment accuracy tolerance of approximately ±0.25mm. Operation near the penetration limit left little spare capacity for coping with effective increases in section thickness arising from surface mismatch or weld closure where the beam had to over-run the reinforcement of the weld start. The situation was considerably eased in the case of the 17mm wall thickness, and Figure 3 shows a typical weld cross section.

The sidehand weld of Figure 3 shows evidence of slumping of the crown under the influence of gravity. We make the simplified assumption that on the pipe surface the melt is bounded by a hemispherical skin of diameter d equal to the crown width and that to avoid drop-out the maximum hydrostatic pressure in the melt, ρgd, must be balanced by the average surface tension pressure which has a maximum value $\pi d\gamma/\grave{}\,\pi d^2$.

Therefore $d^2 \leqslant 4\gamma/\rho g$, where ρ = melt density, 8×10^3kgm^{-3}
γ = surface tension, 1.8 Nm^{-1}
g = acceleration of gravity, 9.8ms^{-2}

The numerical values predict $d \leqslant 9.6$mm which is in remarkably exact agreement with the observed bead width. Although there is evidence of slumping, it did not result in undercutting of the weld crown.

Defects

Self consistent observations by radiography, metallography and visual inspection revealed four defect types, most of which are believed to be associated with operation close to the penetration limit. These were: local disruption of the weld crown, lack of penetration at the root, undercutting at the root, and microporosity. The first occurred in a few instances when, for example, the finely-adjusted gas jet suffered thermal damage so that the gas flow was deflected and displaced molten metal. Additionally, it was noted that the metal flow characteristics were rather different when the girth weld passed through a longitudinal weld. The effect, presumably associated with local compositional variation, requires further investigation; chemical analysis of the longitudinal seam weld revealed an oxygen level of 500ppm which experience suggests can give problems in eb and laser welding. Lack of penetration at the root was clearly a result of operating with insufficient spare capacity. Undercutting at the weld root probably had a similar origin, but it may have been exacerbated by a build up of slight over-pressure within the clamped assembly during welding. The observed microporosity can be classified under two categories: (i) on-axis, often located close to the weld root, with typical pore diameter 0.5mm, predominantly found in welds of rather marginal penetration; (ii) scattered but often located on the fusion boundary, typical pore diameter 0.2mm, widely encountered by metallography. Both categories are characteristic of the laser welding process. The first is almost certainly associated with the solidification of an unstable, blind or near-blind keyhole and is largely absent in welds having generous penetration and a well-vented keyhole. In the present work, intermittent penetration in places in the 19mm material led to a corresponding distribution, on the radiographs, of pores having average separation approximately 5mm; on the other hand, radiographs of welds in 17mm material which had full penetration showed a negligble frequency of this porosity. During ramp-out the weld keyhole must become blind and in this work its instability resulted in micropores on the locus of the withdrawing root. The microporosity of the second category is encountered in the high intensity laser welding of different materials, including Zircaloy[6], and its origin is not at present well understood; its fine scale suggests that its effect on mechanical properties will be minimal.

Tensile, Nick-break and Bend Tests

Test specimens were taken from each quadrant of each of six sample welds. The tensile specimens were machined to the specification test width of 25mm over approximately 230mm of their length; the original pipe surfaces were left as welded i.e. the specimens retained the weld reinforcement at the root and crown of the weld. In all cases fracture occurred in the pipe material with a fracture profile typical of that found in hot rolled plate. The average values of UTS and elongation were 559MPa and 15% respectively, i.e. within X60 parent plate specification.

The nick-break specimens were of similar size to the tensile specimens, and were saw-notched at the weld centre-plane on three faces before being broken. All but one of the 24 specimens fractured on the weld axis. The fracture surface showed complete penetration and fusion as required by the specification. Some microporosity was seen as noted above.

In the case of the side-bend test, two specimens were taken from each quadrant. They were 12.7mm wide x 230mm long and were bent through 180° around a plunger of 25mm radius. In only two out of the 32 specimens the test revealed defects, associated with lack of fusion at the root of the weld, and of depth approximately 1.6mm which lies within the specification maximum defect size of 3.17mm.

Microstructure and Hardness

The micrograpn shown in Figure 4 is of a weld in 17mm wall thickness (11kW, 6mms^{-1}) and is fairly typical. The microstructures were largely of ferrite with aligned MAC[10] and some grain-boundary ferrite, ferrite-carbide aggregates and martensite. Not surprisingly, the parent plate inclusion morphology is greatly altered in the weld. The prior fine stringers, elongated in the rolling direction, have become spherical in the weld melt.

Vickers hardness measurements were carried out in the weld, heat-affected zone (HAZ) and parent plate. In the weld and pipe the indentor loads used were 10 and 30kg, and in the HAZ the loads were 5 and 10kg. The results are presented in Table 2 where it is seen that representative average values of hardness in weld, HAZ and parent are 267, 224 and 188HV respectively. In view of the high quench rates associated with the low heat input of the welds (nominally 2kJmm^{-1}), the value of 267HV does not appear excessively high. However, it lies in a hardness range where careful consideration is required of the possible susceptibility of the weld to stress corrosion and hydrogen induced cracking in an H_2S environment ('sour-gas' condition).

Impact Resistance

Two pairs of standard 10mm x 10mm Charpy V notch specimens were machined transverse to the weld from each pipe sample, one of the pair having the notch in the weld and the other in the HAZ. All notches were cut normal to the plate surface, and the testing was carried out at 21°C. The results are given in Table 2 where it is seen that there is a large amount of scatter on the values for the weld region. The distribution shows the most probable value lies in the range 50-54J which is taken as representative. There is proportionately less scatter in the values for the HAZ, and that distribution shows the most probable value in the range 110-114J. Also given in Table 2 are impact energies for the parent plate where, in relation to the rolling direction, the specimen was oriented (i) transverse i.e. the fracture was longitudinal, (T-L) and (ii) conversely, (L-T). Very consistent results were obtained from several specimens and the representative values were 86J and 121J respectively.

Further sets of specimens were taken from the 17mm pipe weld No. 222 in order to establish ductile/brittle transition curves for the weld and HAZ. The results are shown in Figure 5 together with those for a weld sample after it had received post weld heat treatment (PWHT) at 700°C for 30 minutes. The figure shows also the line for the parent plate L-T and T-L data. In some of the specimens, the fracture deviated out of the weld zone and the resulting high impact energies have not been plotted. The weld metal curve shows impact energy falling from approximately 50J at 21°C to 25J at -10°C. For comparison, it is reported[3] that the specification for the pipeline from the Frigg Field to Scotland called for 40J at -10°C. The PWHT has improved the weld considerably and approximately 55J is achieved at -10°C. The HAZ results appear highly satisfactory, 40J being attained at -60°C. However, the thermal cycle is not very practical from a production point of view and it would also cause down-grading of the parent material.

A short investigation was carried out to determine the potential for improving toughness by control of microstructure via the higher cooling rates obtainable at higher welding speeds. Laser melt runs were carried out at 9.2kW in flat coupons of the same composition, for thicknesses of 12.5mm and 16.5mm, and at speeds of 4, 8 and 15mms^{-1}. Plasma broadening of the weld crown at slow speed meant that the shape of the weld cross section changed strongly over the speed range and quantitative estimates of the variation of cooling rate were difficult. Nevertheless, the microstructures showed, with increasing speed, a higher degree of refinement, decrease in pro-eutectoid ferrite, and increase in martensite. The Charpy transition curves are shown in the left hand side of Figure 6. Again there is considerable scatter, and results in which the fracture deviated have not been plotted. The lines on the figure are sketched to illustrate the trends where it is seen that for a given speed somewhat higher impact values are obtained in the thinner plate and that for both plates, there is a strong improvement with higher welding speed. The right-hand side of Figure 6 shows the variation of impact energy at 0°C, derived from the lines on the left, with welding speed. Also plotted is the weld centre-line hardness measured with a 5kg load. Both properties increase together, in agreement with experience of electron-beam welding of pipe-line steels[3].

Conclusions

This paper has concentrated on describing a welding programme which utilised the CL10 laser prior to full optimisation of its output beam quality, and on reporting the properties of pipe welds carried out in J-lay configuration. In particular, six pipe samples of 760mm diameter and of wall thickness 17mm and 19mm were produced by single pass welding with 11kW and 6mms^{-1}; these underwent destructive testing and fulfilled successfully the requirements of Section 2.6 of the API 1104 specification which concerns the qualification of welding procedures for pipeline. Nonetheless, operation less close to the penetration limit would have been preferable since observed features such as root microporosity and intermittent penetration would have been almost certainly avoided. A more detailed study is required to establish tolerance boxes for the range of process variables; this would permit more accurate prediction of power/thickness relationships. It should be remembered however that for thick section joining, the present unavailability of very high power laser units may mean that single pass autogeneous welding is not the most appropriate technique, and that multipass, narrow-gap welding may be more suitable[11]. The present programme has identified a need for some process refinement in aspects such as beam ramp-out, and the intersection of the longitudinal pipe seam by the circumferential weld. A more fundamental issue is that of weld impact toughness. The trends seen are in broad agreement with published work on electron- beam welding of pipeline[3], viz. toughness increases with decreasing weld width but there is a corresponding increase in hardness which may be unacceptable from the point of view of stress corrosion and hydrogen induced cracking. Clearly there is scope for further work, for example introducing automatic wire feed to control microstructure or, less desirably from a production view point, altering the chemical specification of the parent plate. The present results indicate that HAZ toughness is unlikely to be a limitation in the use of filler. Whilst discussion of production implementation is outside the scope of this paper, it is clear that careful engineering is needed of the marinised laser (or lasers), optimised beam delivery system and pipe clamp capable of giving the appropriate precision, automated control system (ideally with process feedback), and finally fast NDT of the joint. Against this can be set the potential, demonstrated we believe by this present programme, for the laser to create high integrity welds, without 'upset' or need for vacuum, and at a speed relevant to the industry.

Acknowledgements

The work constituted one phase of a project which was partly funded by Brown and Root Inc (Houston), Fairey Engineering Ltd (Stockport) and Ferranti Industrial Electronics Ltd (Dundee), and their stimulation and financial support is gratefully acknowledged. The participation and co-operation of Lloyd's Register of Shipping Research Laboratory, Crawley in the weld testing is appreciatively acknowledged. The welding programme relied on the contributions of many colleagues within the Laser Applications Group.

References

1. Lebedev, V., Kuchuk-Yatsenko, S. and Krivenko, V., Resistance Flash Butt Welding of Pipelines, Proc. Int. Conf. Pipeline and Energy Plant Piping: Design and Technology, Welding Inst. of Canada, 10-13 Nov 1980.
2. Nicholas, E.D. and Lilly, R.H., Radial Friction Welding, Proc. Symp. Alternative Pipe Joining Methods, Chicago, 23-26 Jan 1978, Institute of Gas Technology, 1978.
3. Sudreau, B.G., de Sivry, B. and Anselme, O.R., Electron Beam Weldability for Deep Sea Pipelines, Proc. 13th Annual Offshore Technology Conference, Houston, 4-7 May 1981.
4. Licensee: Ferranti Industrial Electronics Ltd, Dunsinane Avenue, Dundee DD2 3PN,UK.
5. Kaye, A.S., Delph, A.G., Hanley, E. and Nicholson, C.J., Improved Welding Penetration of a 10kW Industrial Laser, Appl. Phys. Lett. 43 (5) pp412-414, 1 Sept 1983.
6. Hill, M., Megaw, J.H.P.C. and Osbourn, S.J., Potential Uses of Laser Welding and Cutting in the Nuclear Fuel Cycle, Proc. 7th Int. Congress Laser/Optoelectronics in Engineering, Munich, 1-5 July 1985, Ed. Waidelich, W., Springer-Verlag 1986. Also as Culham Preprint CLM-P752.
7. Parrini, C., Banas, C. and de Vito, A., Laser Welding of Pipeline Steels, Proc. Int. Conf. Welding of HSLA (Microalloyed) Structural Steels, Rome, 9-12 Nov 1976, Eds. Rothwell, A.B. and Gray, J.M., ASM, Ohio.

8. Megaw, J.H.P.C., Hill, M. and Johnson, R., Laser Welding of Steel Plates with Unmachined Edges, Proc. Conf. Joining of Metals - Practice and Performance, Warwick, 10-12 April 1981, Institute of Metallurgists. Also as Culham Preprint CLM-P649.
9. Lowry, J.F., Fink, J.H. and Schumacher, B.W., A Major Advance in High-Power Electron-beam Welding in Air, J. Appl. Phys. Vol 47, No. 1, pp95-106, January 1976.
10. Abson, D.J. and Dolby, R.E., A Scheme for the Quantitative Description of Ferrite Weld Metal Microstructures, Weld. Inst. Res. Bull., Vol. 21, April 1980.
11. Megaw, J.H.P.C. and Hill, M., Laser Welding of Structural and Stainless Steels, Proc. Int. Conf. on Applications of Lasers and Electro-Optics (ICALEO), Boston, Sept 1982, Vol 31, p108, Laser Institute of America.

Table 1. Compositional Specification & Analysis of API 5LX X60 Steel (Wt. %)

	C	Mn	Si	P	S	Cr	Mo	Ni	Other		O	N
Specification (composition maxima)	0.26*	1.35		0.04	0.05				Nb$^+$ 0.005 V$^+$ 0.02 Ti$^+$ 0.03			
Analysis	0.13	1.48	0.27	0.02	0.007	0.02	0.01	0.03	Nb 0.03 V 0.03 Ti <0.005	Al 0.05 Sn 0.02 Co <0.005 Cu 0.03	0.009	0.015

*For each reduction of 0.01% below maximum specified, an increase of 0.05%Mn above maximum is permissible.
$^+$Either Nb, V, Ti or a combination thereof may be used.

Table 2. Hardness and Charpy Impact Energy Results

Weld No	Wall (mm)	Power (kW)	Speed (mms^{-1})	HARDNESS				CHARPY ENERGY (J) at 21°C	
				WELD		H.A.Z.		WELD	H.A.Z.
				HV$_{10}$	HV$_{30}$	HV$_5$	HV$_{10}$		
219	17	11.0	6	260-274	253-255	203-244	209-247	45, 51, 165	107, 112, 114
220	17	11.0	6	279-287	283-286	210-241	210-243	46, 75, 100	91, 116, 140
221	19	11.2	5	256-285	260-263	216-221	206-238	46, 68, 68	104, 127, 160
222	17	11.0	6	272-279	272-276	219-232	205-243	40, 48, 53	110, 114, 121
233	19	11.4	6	266-297	269-275	236-254	219-243	54, 83, 89	90, 114, 117
224	19	11.4	6	232-253	233-237	195-216	192-227	50, 54, 66	110, 118, 126
Representative values				267HV		224HV		50-54J	110-114J

PARENT PLATE HARDNESS	180-202HV$_{30}$, 170-198HV$_{10}$ AVERAGE 188HV

PARENT PLATE CHARPY IMPACT ENERGY	(L-T)	121J
	(T-L)	86J

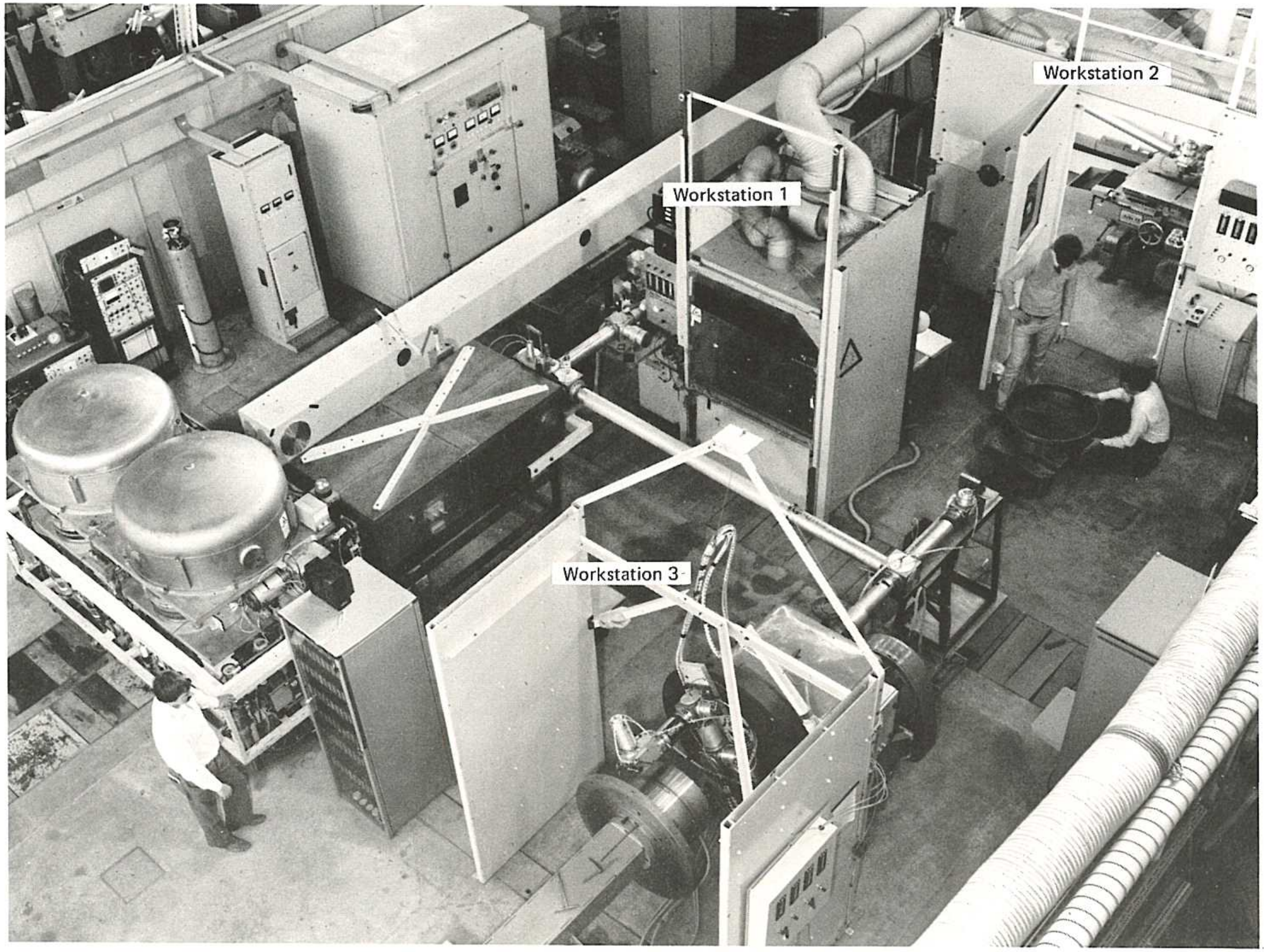
Workstation 2
Workstation 1
Workstation 3

Fig. 1 CL10 Laser Area.

CLM-P773

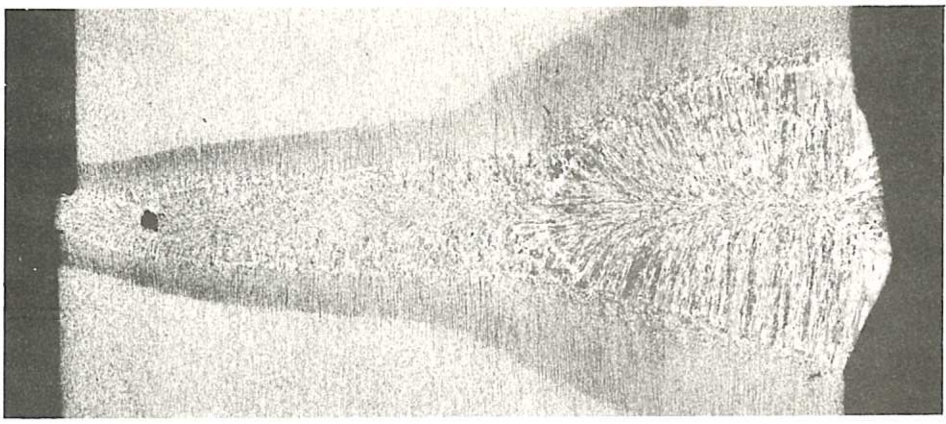

Fig. 2 Laser weld in 19mm thickness.

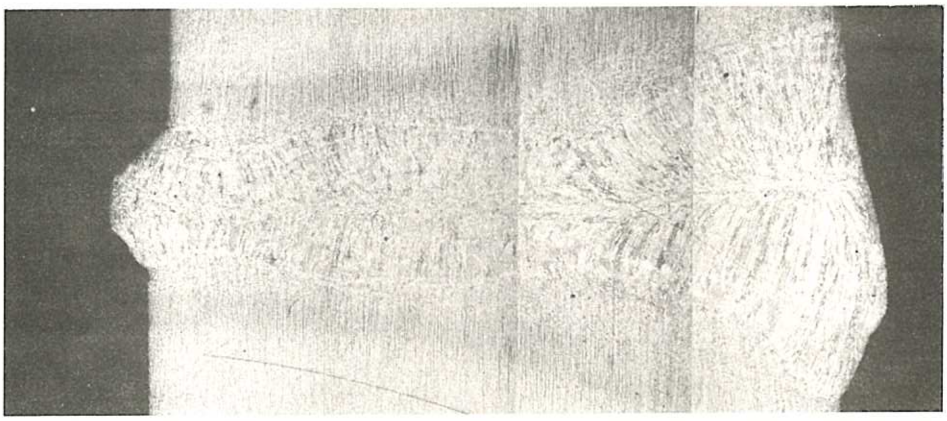

Fig. 3 Laser weld in 17mm thickness.

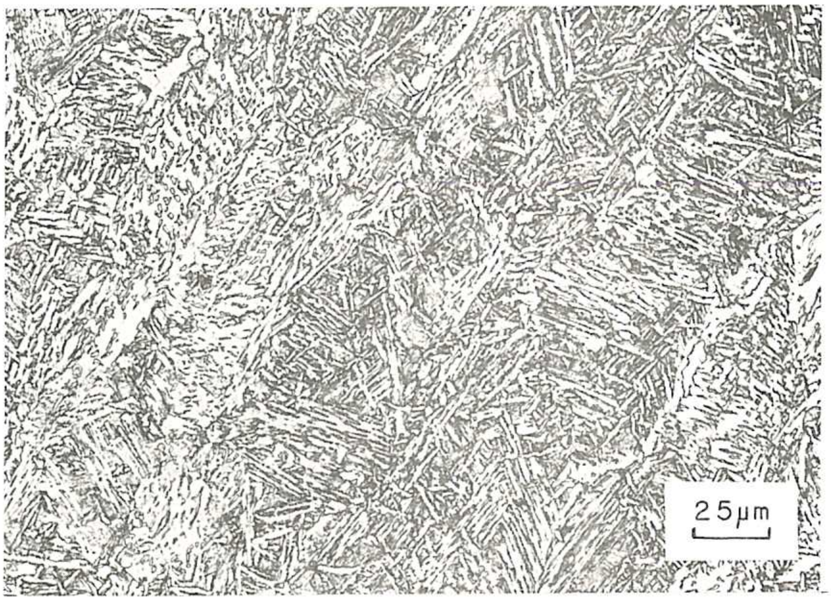

Fig. 4 Weld microstructure.

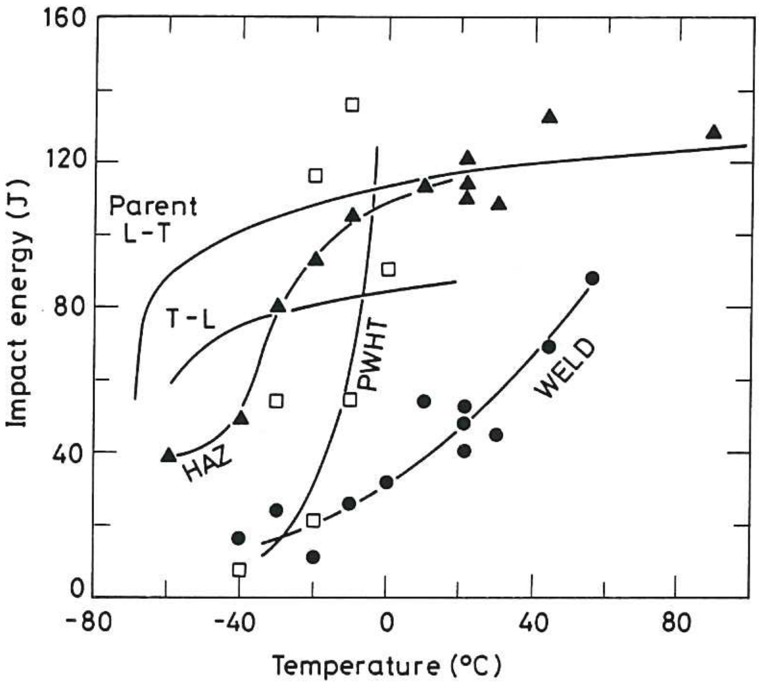

Fig. 5 Charpy impact transition curves.

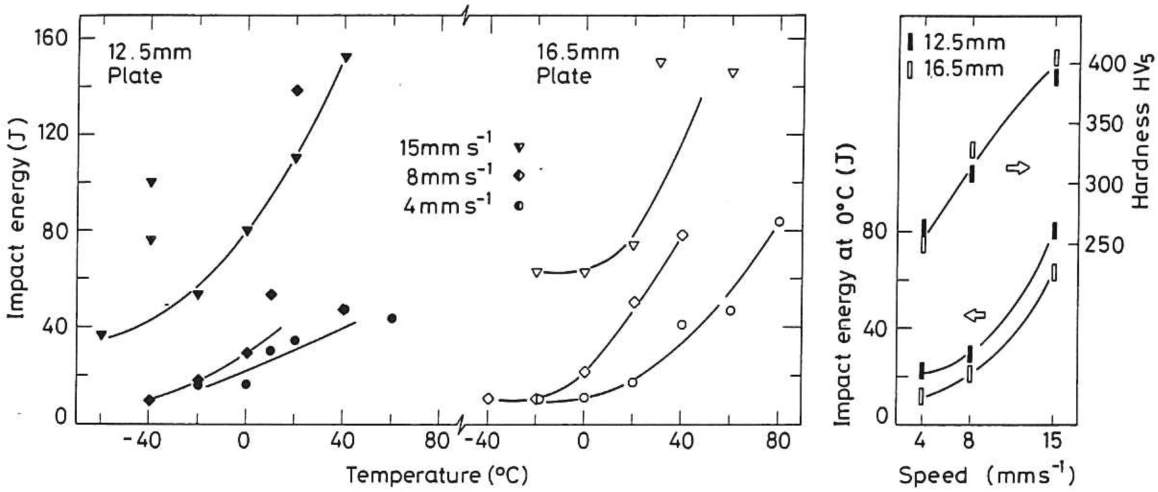

Fig. 6 Variation of weld impact properties and hardness with thickness and speed.